Synthesis and Structures of Dimethyldihydropyrene Iron Carbonyl Complexes

Rui Zhang,[†] Wei Fan,[†] Brendan Twamley,[‡] David J. Berg,*[,†] and Reginald H. Mitchell*[,†]

Department of Chemistry, University of Victoria, P.O. Box 3065, Victoria, British Columbia, Canada V8W 3V6, and the University of Idaho, Moscow, Idaho, 83844

Received January 5, 2007

Reaction of the Diels−Alder adduct **10** (derived from the aryne **11** of dimethyldihydropyrene (DHP) and furan)[7] with $Fe_2(CO)_9$ at room temperature gave the deoxygenated benzannelated DHP **9** and iron tetracarbonyl complex **6**. However, the same reaction at elevated temperature produced **9** as well as the mono-iron tricarbonyl complex **7**, the bis-iron tricarbonyl complex **8** (12%), and a very small amount of **6**. On heating, complex **6** converts to DHP **9** and complex **7**, but does not form **8**. Likewise DHP **9** does not form from either complex **7** or **8**, and so the latter is formed directly from **10**. The structures of **7** and **8** were determined by X-ray crystallography. The main feature of these molecules is the bending of the DHP rings upon coordination of the iron tricarbonyl groups. These molecules are crowded, with strong interactions found between the carbonyl groups and the internal methyl groups and the *tert*-butyl groups. The π-electron delocalization in the normally aromatic DHP ring has been greatly reduced by the complexation.

Introduction

Benzene itself has a low tendency to form diene-type iron tricarbonyl complexes, and only one example, complex **1**, is known, which was synthesized[1] by the reaction of the tetramethylcyclobutadiene iron tricarbonyl complex and $CF_3C{\equiv}CCF_3$. Its structure was determined by X-ray crystallography in 1977.[1] Extended conjugation appears to make complexation of benzene with iron tricarbonyl groups easier. Addition of a substituent vinyl group provides a more reactive center for initial complexation, such that a stable intermediate, (vinyl)$Fe(CO)_4$, is formed prior to the (diene)$Fe(CO)_3$. In some fused polycyclic benzenoids, the bonds are relatively localized, making complexation easier because the resonance energy lost on coordination is relatively small. Thus the stable iron tricarbonyl complexes **2** and **3** on a terminal ring of anthracene[2] and benzanthracene[3] are isolable. The formation of (naphthalene)-$Fe(CO)_3$, **4**, was first reported by Harper,[4] based on an infrared analysis. However, Manuel[2] later cast doubt on its identity. More recently, our group reported the formation of **5**, in which one $Fe(CO)_3$ group is coordinated on the annulene ring of the benzo[14]annulene,[5] which is thus a higher homologue of naphthalene. However, thus far no crystal structures of any of these iron tricarbonyl complexes have been reported. In this paper, we report the isolation of the three dimethyldihydropyrene (DHP) iron carbonyl complexes **6**, **7**, and **8**, as well as the X-ray crystal structures of **7** and **8**.

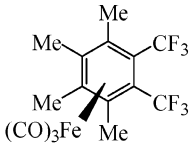

1

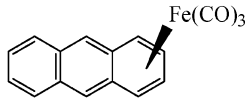

2

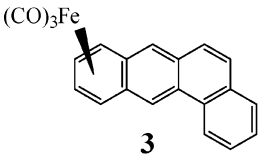

3

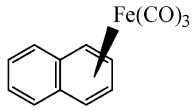

4

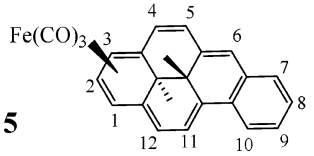

5

Results and Discussion

We have studied extensively the photochromic benzannulene **9**.[6] This is usually prepared by deoxygenation of the adduct **10** (prepared in a Diels−Alder reaction of furan and the aryne **11**[7]) with $Fe_2(CO)_9$. Often however, iron-containing byproducts are formed. A more careful study of this deoxygenation reaction resulted in the isolation of three iron complexes: **6**, **7**, and **8**.

Reaction of adduct **10** with $Fe_2(CO)_9$ at room temperature yielded mostly complex **6** (60%) along with some **9** (20%). On the other hand, reaction in refluxing benzene gave mostly **9** (70%), some mono-iron complex **7** (10%), bis-iron complex **8** (12%), and a very small amount of tetracarbonyl complex **6** (1.5%). This suggested that coordination to the DHP ring proceeds more easily at high temperature.

* Corresponding authors. (D.J.B.) E-mail: djberg@uvic.ca. (R.H.M.) Phone: 250-721-7159. Fax: 250-721-7147. E-mail: regmitch@uvic.ca.
[†] University of Victoria.
[‡] University of Idaho.

(1) Bond, A.; Bottrill, M.; Green, M.; Welch, A. J. *J. Chem. Soc., Dalton Trans.* **1977**, 2372.
(2) Manuel, T. A. *Inorg. Chem.* **1964**, *3*, 1794.
(3) Bauer, R. A.; Fisher, E. O.; Kreiter, C. G. *J. Organomet. Chem.* **1970**, *24*, 737.
(4) Harper, R. J. (Ethyl Corporation) U.S. Patent 3,073,855, Jan 15, 1963.
(5) Mitchell, R. H.; Zhou, P. *Angew. Chem., Int. Ed. Engl.* **1991**, *30*, 1013.
(6) Mitchell, R. H. *Eur. J. Org. Chem.* **1999**, 2695.
(7) Mitchell, R. H.; Ward, T. R. *Tetrahedron* **2001**, *57*, 3689.

10.1021/om0700112 CCC: $37.00
Publication on Web 03/13/2007

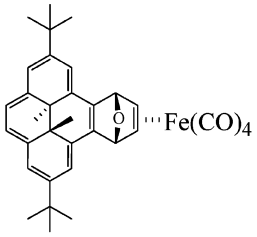

6

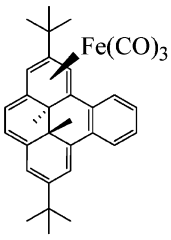

7

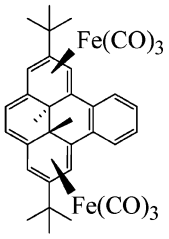

8

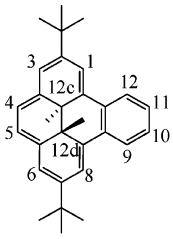

9

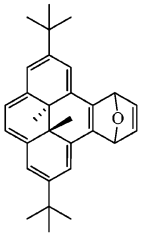

10

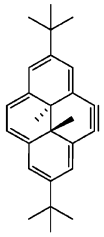

11

The structures of **6**, **7**, and **8** were determined from their ^{1}H NMR, ^{13}C NMR, mass, and IR spectra. As well, X-ray structures were obtained for **7** and **8**. In their IR spectra, the carbonyl stretches were all strong. For **6**, they appear at 2082, 2021, 1991, and 1968 cm^{-1}, consistent with those for the analogous epoxynaphthalene derivative[8a] at 2085, 2020, 2010, and 1985 cm.$^{-1}$ For **7**, the carbonyl stretches are at 2032, 1977, and 1954 cm^{-1}, which are at lower frequency than those[8b−d] for butadiene irontricarbonyl at 2054, 1988, and 1978 cm.$^{-1}$ This is consistent with substantial donation of electron density from the 14π-ring into the iron tricarbonyl fragment.

The ^{1}H NMR spectrum of **6** shows the DHP peripheral proton resonances in the typical DHP region (δ 8.31−8.22). The internal methyl protons appear at δ −3.01 and −3.17, which are again typical for a DHP, and so both sets of protons indicate the presence of a strong ring current. This suggests that the site of complexation is not directly on the DHP ring. The coordination position of the iron tetracarbonyl was indicated by the shielded chemical shifts of the bridging ethene protons H-10 and H-11 at δ 3.29 and 3.04, relative to their shifts of δ 7.12 in **10**. The bridgehead ether hydrogens, H-9 and H-12, are both singlets at δ 5.97 and 5.92, respectively. Since protons H-10 and H-11 are doublets, while H-9 and H-12 are singlets, the fused six-membered ring is most likely bent along the C-9$\cdots$C-12 axis, such that the H-9−C-9−C-10−H-10 dihedral angle is about 90°. Then the coupling between H-9 and H-10 (and likewise between H-12 and H-11) would be very small. The ^{13}C NMR spectrum showed all the expected carbon signals with the carbonyl carbon at δ 211.8 and the coordinated C-10 and C-11 carbons at δ 59.6 and 59.5, shielded due to complexation. The bridgehead ether carbon atoms (C-9 and C-12) appear at δ 81.43 and 81.38. Finally the structure of **6** was further confirmed by $^3J_{H,C}$ couplings between H-12 and C-9 and also between H-9 and C-12 in their ^{1}H−^{13}C HMQC spectra, which would not be possible in the absence of the ether bridge. The LSI and the high-resolution mass spectra confirmed the structure of **6** to be a tetracarbonyl.

The chemical shifts for the internal methyl protons of **7** appeared at δ 2.01 and 2.47, which are similar to those found in **5**, the analogous [*a*]-fused benzoDHP tricarbonyl iron complex (δ 2.00, 1.71).[7] Such chemical shift values indicate that the coordination of the Fe(CO)$_3$ moiety is on the DHP ring and not on the benzenoid ring, in which case a value close to that of **12** (δ −4.2) would have been expected. The position of complexation in **7** is evident from the shielded chemical shift of H-3 (δ 3.67), the proton at the end of the complexed diene unit. The ^{13}C NMR spectrum of **7** clearly shows the carbonyl carbon signals at δ 212.3 and the four upfield carbon signals (δ 64.1−108.5) of the complexed diene unit. The structure of **7** was finally confirmed by a single-crystal X-ray structure determination (discussed below).

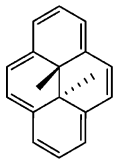

12

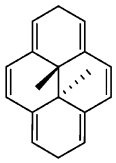

13

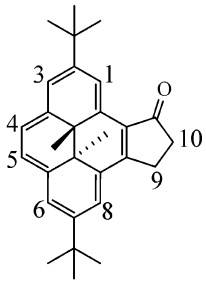

14

The fact that the chemical shifts of the internal methyl protons of **7** are close to those of **5** and that both are more deshielded than those of the nonaromatic model **13** (δ 0.97) is interesting. In **5**, we attributed[5] these deshielded internal methyl protons to a weakly paratropic ring current due to the back-donation of two electrons by iron to the 14π system to form an antiaromatic 16π system. This conclusion was supported by the fact that the chemical shifts of *all* the protons in the fused benzene ring (δ 6.77−7.24 in $CDCl_3$) were shielded when compared to those in benzene itself (δ 7.36 in $CDCl_3$). As well, the coupling constants ($J_{7,8}$ = 7.5 Hz, $J_{8,9}$ = 7.4 Hz, $J_{9,10}$ = 7.6 Hz) of the fused benzene ring were almost equal, which indicates that any ring current in the large ring is small. It is not quite so obvious whether **7** is behaving similarly. First, two of the protons on the fused benzene ring, H-9 and H-12 at δ 7.42 and 7.19 in C_6D_6, are deshielded somewhat compared to benzene itself (δ 7.15 in C_6D_6). This may be in part due to steric deshielding of the bay protons. The other two protons, H-10,11, are shielded at δ 6.91 and 6.97. Second, the coupling constants in the fused benzene ring of **7** appear to alternate more, with $J_{9,10}$ = 8.0 Hz, $J_{10,11}$ = 7.0 Hz, and $J_{11,12}$ = 8.1 Hz, though again these can be affected by steric compression. One would expect the geometries of **7** and **5** to be somewhat different, because the complexed end of the dihydropyrene in **7** is obviously more crowded than that in **5**. Unfortunately, no crystal structure of the [*a*]-complex **5** is available, but we have performed DFT (B3LYP/6-31G*) calculations[9] on both it and **7** and **8** (since we have X-ray structures of the latter two, which will enable us to assess the goodness of the calculations. In all three cases, the calculations suggest that most of the dihydropyrene framework is relatively flat, with the plane of the carbon atoms of the complexed diene part (e.g., C-1,2,3,3a in structure **5**) bent out of the plane formed by the central atoms (e.g., C-3a,4,5,-5a,10b,11,12,12a in structure **5**) of the DHP ring. For compound **5**, this angle between the planes is 28.9°. From a p-orbital overlap point of view, the worst misalignment is between atoms

(8) (a) Lombardo, L.; Wege, D.; Wilkinson, S. P. *Aust. J. Chem.* **1974**, *27*, 143. (b) Lokshin, B. V.; Klemenkova, Z. S.; Rybin, L. V.; Aleksanyan, V. T. *Izvest. Akad. Nauk SSSR, Ser. Khim.* **1981**, *5*, 989. [CAN 95:123168, AN 1981:523168]. (c) Bachler, V.; Grevels, F-W.; Kerpen, K.; Olbrich, G.; Schaffner, K. *Organometallics* **2003**, *22*, 1696. (d) Davidson, G. *Inorg. Chim. Acta* **1969**, *3*, 596.

(9) *Spartan 06*, V1.0.2; Wavefunction, Inc: Irvine, CA 92612, 2006.

Table 1. Summary of Crystallographic Data

	7	**8**
formula	$C_{33}H_{34}FeO_3$	$C_{36}H_{34}Fe_2O_6$
fw	534.45	674.33
cryst syst	monoclinic	orthorhombic
space group	*P*2(1)/*n*	*Pbca*
a (Å)	10.3156(7)	16.2931(7)
b (Å)	13.1485(9)	18.4265(8)
c (Å)	19.4451(13)	20.3460(9)
α (deg)	90	90
β (deg)	91.235(1)	90
γ (deg)	90	90
V (Å^3)	2636.8(3)	6108.4(5)
Z	4	8
ρ(calcd) (Mg/m^3)	1.346	1.467
abs coeff (mm^{-1})	0.605	0.997
F(000)	1128	2800
θ range for data collection (deg)	1.87 to 25.24	1.95 to 25.25
no. of reflns collected	35 854	93 472
no. of indep reflns	4778 [*R*(int) = 0.0289]	5529 [*R*(int) = 0.0410]
completeness to *θ*	25.24°, 99.9%	25.25°, 100.0%
no. of data/restraints/params	4778/0/342	5529/0/405
goodness of fit on *F*^{2}	1.099	1.067
final *R* indices [$I > 2\sigma(I)$][a]	R1 = 0.0381 wR2 = 0.0971	R1 = 0.0378 wR2 = 0.0916
R indices (all data)[a]	R1 = 0.0410 wR2 = 0.0988	R1 = 0.0414 wR2 = 0.0940

[a] $R1 = \sum||F_o| - |F_c||/\sum|F_o|$; $wR2 = \{\sum[w(F_o^2 - F_c^2)^2]/\sum[w(F_o^2)^2]\}^{1/2}$.

3, 3a, and 4 (∼24°), which is not exceptionally bad in terms of ring current effects.[10] The ^{1}H NMR data then suggest that the *π* electrons in the DHP ring of **5** are still delocalized and show a weak paratropic ring current. In the [*e*]-complex **7**, the angle between the corresponding planes (above) to **5** is almost the same, 29.3° by DFT calculation and 30.7° from the X-ray structure (see below). Repeating the calculation for **5** with a *tert*-butyl substituent at the 2-position does not significantly (<0.5°) change this situation. Comparison of the calculated and experimental structures for **7** gives excellent agreement (see Table 2 below), as they do for **9** and **12** (see below), and so it seems reasonable that both **5** and **7** are behaving similarly and both show a small paratropic ring current, explaining why the chemical shifts for the internal methyl protons for both compounds are more deshielded than those of the nonaromatic **13**. However, anisotropy effects must also play a roll, since the internal methyl protons that are *cis* to the $Fe(CO)_3$ group are very close to one of the CO groups, while the *trans* internal methyl protons are close to the complexed diene. Both groups have deshielding regions, which must impact the observed chemical shifts. We have observed previously that for **14** H-1 is about 1 ppm further downfield than H-8.[11] The observed variation in the chemical shifts of the internal methyl groups in **5** and **7** may then reflect these anisotropies, rather than a substantial difference in ring current.

For complex **8**, similar to **7**, the downfield chemical shifts for the internal methyl protons suggest only a small ring current and imply the loss of aromaticity of the macro-ring on the coordination of the two $Fe(CO)_3$ groups. In this case, the chemical shift difference between the two internal methyl groups is quite large ($\Delta\delta = 1.47$) compared to that for **7** ($\Delta\delta = 0.46$). This suggests that the two internal methyl groups have rather different environments and implies that the two $Fe(CO)_3$ groups are coordinated on the same side of the DHP ring. This was actually confirmed by a single-crystal X-ray structure, which is discussed below. Similar to complex **7**, the downfield chemical shifts of protons H-3 (*δ* 3.78) and H-6 (*δ* 3.89) reveal the position of the complexation.

Although it has been reported by our group[5] that **5** can be synthesized by direct reaction of the benzo[*a*]DHP with $Fe_2(CO)_9$ in refluxing benzene, no reaction was found between benzo[*e*]DHP **9** and $Fe_2(CO)_9$, $Fe(CO)_5$, or $Fe_3(CO)_{12}$ under similar conditions. This suggests that complexes **7** and **8** are formed before or during the deoxygenation process and not after it.

The tetracarbonyl **6** is not thermally stable and at room temperature slowly loses iron and forms DHP **9**. At elevated temperatures it converts more quickly to **9** and also forms some complex **7** in a ratio of 2.3 to 1. For example, in refluxing benzene for 2 h, over 90% of **6** has been converted to **9** and **7**. The half-life of **6** in refluxing benzene is about 30 min. This explains the high yield of **6** at room temperature, and the lower yield at elevated temperature, when it decomposes to **9** and **7**. It also explains the higher yield of **9** at higher temperature. However, no di-iron complex **8** was detected in this process. Since no reaction was found between **7** and $Fe_2(CO)_9$ in refluxing benzene, we conclude that **8** must have formed directly from the reaction of **10** and $Fe_2(CO)_9$.

Thermal study of **7** and **8** found that **7** slowly loses the $Fe(CO)_3$ moiety to form **9** at elevated temperatures. For example, refluxing in benzene for 2 h converts several percent of **7** to **9**. Similarly, **8** first loses one $Fe(CO)_3$ to form **7**, which then continues to lose another $Fe(CO)_3$ to form **9**, but at a much slower rate.

All of the above results support a mechanism for the reaction of **10** and $Fe_2(CO)_9$ that proceeds via one or more intermediate states, which can directly decompose to the deoxygenated product **9** or react with $Fe_2(CO)_9$ to form the iron complexes.

Crystal Structure of 7. The crystal structure of **7** is shown in Figure 1. The crystallographic data are summarized in Table 1, and selected bond lengths are given in Table 2. Selected bond angles are in Table S1 (Supporting Information). Clearly, coordination has occurred on one side of the DHP ring such that the $Fe(CO)_3$ group is furthest away from an internal methyl group, i.e., on the same side as C(26) in Figure 1, rather than on the side of C(24). The main feature of **7** is the bending of the DHP ring. The angle between the planes defined by the four carbon atoms of the complexed diene (C(7)−C(6)−C(5)−C(22), Figure 1) and the central carbon atoms of the DHP (C(22) to C(18), C(14)−C(13), and C(8)−(C7), Figure 1) is 30.7°, which is smaller than but similar to those of compounds related to (1,3-cyclohexadiene)$Fe(CO)_3$ (36.3−39.9°)[12] and also smaller than those of other η^4-arene complexes (37.4−47.9°),[13] but as mentioned above, agrees very well with a DFT (B3LYP/6-31G*)[9]-calculated value of 29.3°.

The butadiene iron tricarbonyl portion of the molecule shows typical characteristics of all (butadiene)$Fe(CO)_3$ complexes. For example, the four carbon atoms of the diene unit are planar. The iron atom is closer to the inner carbon atoms (C(5), C(6))

(10) (a) Haddon, R. C.; Scott, L. T. *Pure Appl. Chem.* **1986**, *58*, 137. (b) Mitchell, R. H. *Adv. Theor. Int. Mol.* **1989**, *1*, 135.

(11) Mitchell, R. H.; Fan, W.; Lau, D. Y. K.; Berg, D. J. *J. Org. Chem.* **2004**, *69*, 549.

(12) Deeming, A. J. *Comprehensive Organometallic Chemistry*; Pergamon Press Ltd: New York, Wilkson, G., Stone, G. A., Abel, E. W., Eds.; 1982; Vol. 4, Chapter 31.3, p 377.

(13) (a) Albright, J. O.; Brown, L. D.; Datta, S.; Kouba, J. K.; Wreford, S. S. *J. Am. Chem. Soc.* **1977**, *99*, 5518. (b) Albright, J. O.; Datta, S.; Dezube, B.; Kouba, J. K.; Marynick, D. S.; Wreford, S. S.; Foxman, B. M. *J. Am. Chem. Soc.* **1979**, *101*, 611. (c) Gladfelter, W. L.; Hull, J. W. *Organometallics* **1984**, *3*, 605. (d) Schaufele, H.; Hu, D.; Pritzkow, H.; Zenneck, U. *Organometallics* **1989**, *8*, 396.

Table 2. Selected Experimental (exp) and Calculated [DFT B3LYP/6-31G*][9] (calc) Bond Lengths (Å) for Complexes 9,[20a] 7, and 8

	9		7		8	
bond[a]	exp	calc	exp	calc	exp	calc
C(5)−C(22)	1.354(4)	1.377	1.447(3)	1.445	1.440(3)	1.512
C(5)−C(6)	1.440(4)	1.442	1.405(3)	1.422	1.422(3)	1.349
C(6)−C(7)	1.362(3)	1.366	1.431(3)	1.431	1.427(3)	1.512
C(7)−C(8)	1.463(4)	1.459	1.484(3)	1.491	1.491(3)	1.498
C(8)−C(9)	1.413(4)	1.418	1.404(3)	1.408	1.400(3)	1.406
C(9)−C(10)	1.362(4)	1.380	1.381(3)	1.389	1.379(3)	1.390
C(10)−C(11)	1.397(4)	1.406	1.391(3)	1.397	1.389(3)	1.396
C(11)−C(12)	1.363(4)	1.380	1.380(3)	1.387	1.382(3)	1.391
C(12)−C(13)	1.411(4)	1.418	1.407(3)	1.409	1.398(3)	1.404
C(13)−C(14)	1.450(4)	1.459	1.480(3)	1.477	1.493(3)	1.500
C(14)−C(15)	1.364(3)	1.366	1.347(3)	1.355	1.420(3)	1.415
C(15)−C(16)	1.437(4)	1.442	1.469(3)	1.463	1.422(3)	1.432
C(16)−C(17)	1.359(4)	1.377	1.355(3)	1.365	1.448(3)	1.464
C(17)−C(18)	1.429(4)	1.420	1.439(3)	1.438	1.461(3)	1.455
C(18)−C(19)	1.367(4)	1.378	1.357(3)	1.366	1.349(3)	1.372
C(19)−C(20)	1.429(3)	1.423	1.449(3)	1.450	1.455(3)	1.447
C(20)−C(21)	1.351(4)	1.378	1.353(3)	1.358	1.351(3)	1.385
C(21)−C(22)	1.431(3)	1.420	1.450(3)	1.458	1.449(3)	1.425
C(8)−C(13)	1.426(3)	1.377	1.423(3)	1.430	1.426(3)	1.438
av C−C (DHP)	1.4044	1.4101	1.4206	1.4249	1.4324	1.4431
av C−C (Benz)	1.3953	1.4060	1.3977	1.4033	1.3957	1.4042
av dev C−C (DHP)	0.0385	0.0312	0.0409	0.0369	0.0300	0.0409
av dev C−C (Benz)	0.0219	0.0173	0.0137	0.0123	0.0123	0.0119
C(5)−Fe(1)			2.064(2)	2.080	2.065(2)	2.870
C(6)−Fe(1)			2.057(2)	2.066	2.059(2)	2.879
C(7)−Fe(1)			2.265(2)	2.266	2.282(2)	2.193
C(22)−Fe(1)			2.147(2)	2.147	2.171(2)	2.049
C(14)−Fe(2)					2.262(2)	2.318
C(15)−Fe(2)					2.068(2)	2.088
C(16)−Fe(2)					2.039(2)	2.023
C(17)−Fe(2)					2.167(2)	2.174

[a] X-ray numbering.

than the outer ones (C(7), C(22)), and the inner C(5)−C(6) bond is shorter than the outer C(5)−C(22) and C(6)−C(7) bonds. The three CO groups are not equivalent, with one CO group lying over the "open" side of the *cis*-C−C−C−C chain, while the other two lie over the outer C−C bonds. The arrangement of the ligands can thus be described as square pyramidal with the C(33)−O(3) group forming the quasi-4-fold axis and the other two CO groups and the midpoints of the outer C(5)−C(22) and C(6)−C(7) bonds forming the basal square. This is a typical stereochemistry for this type of compound. The bite angle of 61.1° for the complexed diene is normal.

However, because of the presence of the *tert*-butyl and internal methyl groups, the molecule is crowded at the complexed end of the DHP framework. The shortest contacts are found between C(31)···H(1C), C(33)···H(26A), and C(33)···H(26B) with distances of 2.578, 2.613, and 2.696 Å, respectively, which are all shorter than the sum of van der Waals radii of hydrogen and carbon atoms (2.9 Å). To avoid space conflicts with the *tert*-butyl protons, the Fe(1)−C(31)−O(1) (175.5°(2)) is bent away from linearity and C(1) and C(2) of the *tert*-butyl group are pushed away from the metal center with the C(1)−C(4)−C(5) and C(2)−C(4)−C(5) angles being 112.0(2)° and 113.7(2)°, respectively, away from ideal tetrahedral geometry. The quaternary *tert*-butyl carbon (C(4)), however, is only 0.235 Å away from the complexed diene plane and does not deviate much from coplanarity with the diene plane. Similarly the interactions between the C(33)−O(3) group and the *cis*-internal methyl protons (H(26A) and H(26B)) push C(33) toward C(31) and result in a tilt of the internal methyl carbon (C(25)) away from the iron center with the C(23)−C(25)−C(26) angle being 114.8(2)°. Thus the C(33)−Fe(1)−C(31) angle is only 91.5(1)°, significantly smaller than the values (95−103°)[12] found in other (butadiene)$Fe(CO)_3$ complexes, and the Fe(1)−C(33)−O(3) angle is only 172.6(2)°, significantly different from 180°. To relieve the strain in the molecule, the iron atom is also situated further (1.71 Å) from the diene plane than in other butadiene $Fe(CO)_3$ complexes (1.55−1.64 Å).[14,15] This in turn causes longer bond lengths between the iron and the outer carbon atoms. The average of 2.26 Å for Fe(1)−C(7) and Fe(1)−C(22) distances falls well outside of the normal range of 2.10−2.16 Å for (butadiene)$Fe(CO)_3$ complexes.[12] However the bond lengths between the iron and the inner carbon atoms (2.064(2) and 2.057(2) Å) are normal. The average Fe−carbonyl distance of 1.798 Å is comparable with the many reported values

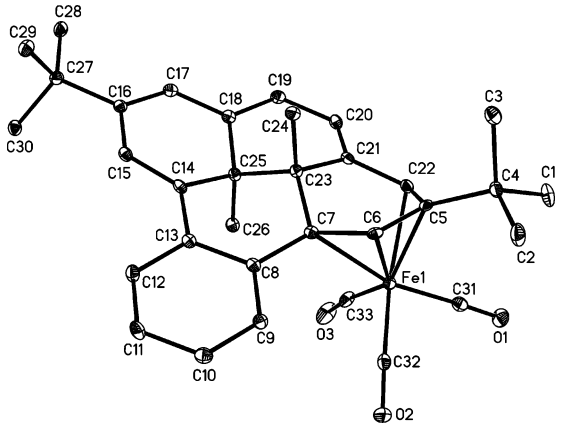

Figure 1. ORTEP3 drawing[17] of complex **7** (30% probability thermal ellipsoids). Hydrogen atoms have been removed for clarity.

(14) Mills, O. S.; Robinson, G. *Acta Crytallogr*. **1963**, *16*, 758.
(15) Cotton, F. A.; Troup, J. M. *J. Organomet. Chem*. **1981**, *212*, 411.

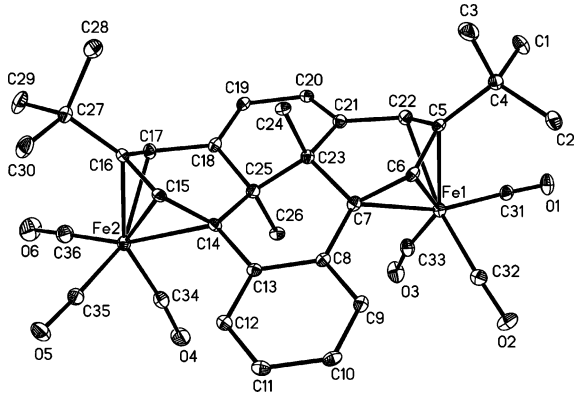

Figure 2. ORTEP3 drawing[17] of complex **8** (30% probability thermal ellipsoids). Hydrogen atoms have been removed for clarity.

(1.75−1.80 Å).[16] Three of the four C−C−C angles in the complexed diene portion are significantly smaller than 120°, which is not common in (butadiene)$Fe(CO)_3$ complexes, but has been observed in η^4-naphthalene complexes before.[13b]

The uncomplexed part of the ligand does not deviate significantly from coplanarity. The largest deviations are found at C(15) (0.195 Å). However, more careful study found that the free *tert*-butyl end of the DHP ring is slightly bent toward the metal center with a dihedral angle of 8.9° between planes defined by C(15)−C(17) and the central part of the ligand (C(7)−C(14) and C(18)−C(22)). The benzene ring retains planarity and is almost bond equal. The bond alternation around the DHP ring is discussed below.

Crystal Structure of 8. The crystal structure of **8** is shown in Figure 2. The crystallographic data are summarized in Table 1, and selected bond lengths are given in Table 2 and bond angles in Table S1 (Supporting Information). The two iron tricarbonyl groups are coordinated to the two butadiene units at the two *tert*-butyl ends and on the same side. The DHP ring is thus bent at both ends, and a boat structure is formed. The central part of the boat structure, a plane defined by C(7)−C(8), C(13)−C(14), and C(17)−C(22), is quite flat, with maximum deviations found at C(20) (0.177 Å), C(18) (0.104 Å), and C(7) (0.090 Å), respectively. The dihedral angles between the two complexed diene planes and the central plane are 31.3° and 51.4°, respectively. The larger angle is for the diene unit, which has the $Fe(CO)_3$ group and the closer internal methyl group on the same side, (i.e., Fe2 and C26 in Figure 2) and is obviously caused by stronger intramolecular interactions. The dihedral angle between the two diene planes is 71.3°.

The two tricarbonyl iron butadiene portions of the molecule show similar structural features to those found in **7**, but show larger molecular distortions. The two iron atoms are 1.713 and 1.726 Å from the diene planes, respectively, similar to that in **7**. The average inner and outer C−C bond lengths are the same for the two complexed diene units. The average inner bond lengths (1.422 Å) are longer and the average outer bond lengths (1.434 Å) are shorter than those of **7** (1.405 and 1.439 Å), suggesting stronger π-back-donation from iron in **7**. Similar to **7**, the shortest intramolecular contacts are found between C(33)···H(26C) (2.453 Å) and C(34)···H(26A) (2.352 Å) on the internal methyl side and C(31)···H(1A) (2.717 Å), C(31)···H(2C) (2.780 Å), and C(36)···H(29C) (2.645 Å) on the *tert*-butyl sides. These data display the congestion in the molecule. They also show that the accommodation of two $Fe(CO)_3$ groups on one side of the DHP ring results in a more crowded environment for the *cis*-internal methyl group compared to that of **7**. Also the Fe−C−O angles in **8** are all significantly smaller than 180°, rather than just some of them as in **7**. This implies a great deal of molecular strain in **8**. The C−Fe−C angles are all similar to those in **7**.

The structure of **8** was a surprise to us, as one might expect that coordination of the two tricarbonyl iron groups on opposite sides of the ligand would cause less strain in the molecule. In that way both of the $Fe(CO)_3$ groups could stay away from the *cis*-internal methyl group, unlike in **8**, where one $Fe(CO)_3$ has to be next to the *cis*-internal methyl. However, calculations of ΔH_f disagree, and a PM3 calculation[9] for **8** and the analogous *trans*-$Fe(CO)_3$ isomer suggests that the *cis*-isomer **8** is more stable by 110 kJ/mol! Of course, it may be that the kinetic approach of the second iron moiety is favored on the outside of the "saucer"-shaped molecule. Interestingly, a similar structure has been observed before in the heptalene bis(tricarbonyliron) system, **15**.[18]

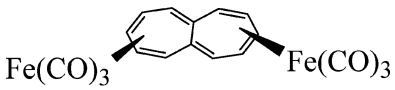

15

Bond Localization Effects. When two annulenes are fused along a common side, bond localization occurs in both rings and leads to alternating bond lengths and coupling constants. The actual bond localization effects depend on the aromaticity or antiaromaticity of each annulene. If one annelated annulene is aromatic and has a large resonance energy, it will cause a large bond fixation on the fused annulene. Antiaromatic annulenes cause the same effect, though the bond alternation pattern is different.[19]

The experimental and calculated bond lengths in the free ligand **9**[20a] and complexes **7** and **8** are given in Table 2. Note that Spartan[9] (DFT, B3LYP/6-31G*) tends to overestimate the average bond lengths 1.4044 (exp DHP), 1.4101 (calc DHP), 1.3953 (exp Benz), and 1.4060 Å (calc Benz) for **9** and also in similar annulenes, and underestimate the average deviation of each bond from the average bond length 0.0385 (exp DHP), 0.0312 (calc DHP), 0.0219 (exp Benz), and 0.0173 Å (calc Benz) for **9**. Nevertheless, the correlations are quite good.[20a−c] This average deviation can be used as a measure of the bond alternation around each ring and in turn as a measure of the size of the ring current.[20a,b]

Both the DHP and the benzene ring in **9** show stronger bond alternation (av dev = 0.0385 and 0.0219, respectively) than in the parent **12** (av dev = 0.0027) or its 2,7-di-*tert*-butyl derivative (av dev = 0.0049), and the ring current in each ring is reduced by about 50%[20b,c] from that of the parents, because both fused rings, DHP and benzene, are strongly aromatic. However, in **7** the DHP ring displays greater alternation (av dev = 0.0409) than in **9**, but the benzene ring (av dev = 0.0137) shows less. This suggests now that the DHP ring in **7** is less aromatic than

(16) Cotton, F. A.; Day, V. W.; Frenz, B. A.; Hardcastle, K. I.; Troup, J. M. *J. Am. Chem. Soc.* **1973**, *95*, 4522.

(17) Farrugia, L. J. *J. Appl. Crystallogr.* **1997**, *30*, 565.

(18) (a) Stegemann, J.; Lindner, H. J. *J. Organomet. Chem.* **1979**, *166*, 223. (b) Müllen, K.; Allison, N. T.; Lex, J.; Schmickler, H.; Vogel, E. *Tetrahedron* **1987**, *43*, 3225.

(19) Cremer, D.; Günther, H. *Justus Liebigs Ann. Chem.* **1972**, *763*, 87.

(20) (a) Williams, R. V.; Armantrout, J. R.; Twamley, B.; Mitchell, R. H.; Ward, T. R.; Bandyopadhyay, S. *J. Am. Chem. Soc.* **2002**, *124*, 13495. (b) Mitchell, R. H.; Williams, R. V.; Mahadevan, R.; Lai, Y. H.; Dingle, T. W. *J. Am. Chem. Soc.* **1982**, *104*, 2571. (c) Mitchell, R. H. *Chem. Rev.* **2001**, *101*, 1301.

Scheme 1

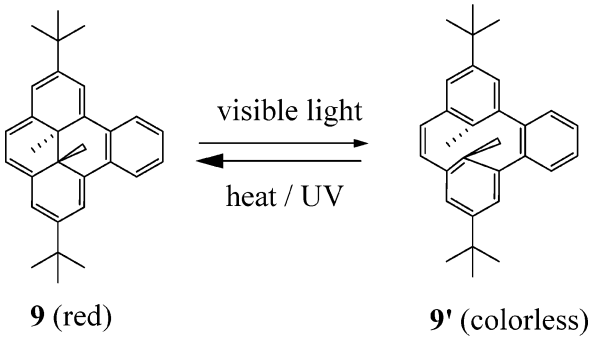

that in **9**. However, this DHP ring must still retain considerable delocalization, since the noncyclically conjugated model **13** has an av dev = 0.0562. Our conclusion then is that this delocalization is contributing to a small paratropic ring current, which would account for the chemical shifts of the internal methyl protons, relative to those in **9**, the weak effect on the benzene ring, and the back-donation of iron suggested from the X-ray structure above. The greater calculated av dev in the benzene ring of **7** (0.0123) than in **5** (0.0092) is consistent with the observed coupling constants for these compounds. Overall, the average carbon−carbon bond length of the dihydropyrene ring increases from **9** to **7** to **8**, consistent with increasing electron withdrawal from the DHP π system by the iron tricarbonyl groups. Interestingly though, the calculations for the bis-iron complex **8** do not agree so well with the X-ray structure. As can be seen from Table 2, the calculated structure has considerably more bond fixation in the DHP ring than is found in the crystal structure. This is especially apparent at the C7−C6−C5−C22 end of the molecule, where the iron tricarbonyl moiety, Fe1 in Figure 2, has slipped toward the methyl group (C26) such that the bonding appears to be ene-diyl; that is, C5−C6 has more double-bond character and C5−C22 and C6−C7 have more single-bond character. The energy well may be rather shallow with a consequence that the crystal structure and calculated structures are not so different in energy. Certainly in solution, the bis-iron complex **8** does not appear to be more delocalized in the DHP ring than the mono-complex **7**, as the crystal structures suggest!

Photoswitching Properties. Both the parent DHP **11** and the benzoDHP **9** are photochromic. Irradiation of a benzene solution of **9** with visible light from a 500 W tungsten lamp, using a 490 nm cut-off filter, quickly converts it to the cyclophane diene (CPD) **9′** (Scheme 1). We were interested in how the coordination of $Fe(CO)_3$ and $Fe(CO)_4$ groups would modify the photochromic properties of DHPs. However, under similar conditions, irradiation of a benzene solution of complex **7** or **8** yielded none of the CPD forms and very little or no decomposition. Irradiation of **6**, on the other hand, resulted in the formation of benzoDHP **9** along with some precipitate. None of the open form of **6** could be detected. It is interesting that no iron complexes of any DHP systems we have made have turned out to be photochromic,[21] while some other metal systems, including those containing Ru,[22] are. The reasons for this are not yet clear, but differences in the ligand field state energies no doubt play an important role, where the first-row transition metals appear to quench the photochemistry.

(21) The $Fe(CPDHP)_2$ and ferrocenyl-substituted Benz or DHP complexes do not photoopen under similar conditions.

(22) Mitchell, R. H.; Brkic, Z.; Sauro, V. A.; Berg, D. J. *J. Am. Chem. Soc.* **2003**, *125*, 7581.

Conclusions

Three iron dihydropyrene complexes have been synthesized, and X-ray structures of two, **7** and **8**, have been obtained. In these two, coordination of the metal occurs on the DHP ring and causes a distortion of about 30° from planarity of the large ring. This ring then shows increased bond alternation and loss of aromaticity relative to the ring in the ligand **9**. Some delocalization however remains, and possibly a paratropic ring current coupled with strong anisotropic effects causes the downfield shifts of the internal methyl protons in **7**. Crystal packing forces may override other considerations in the very crowded **8**, such that the chemical shifts are driven more by anisotropic effects than ring currents. Complexation suppresses the photochromic behavior of the dihydropyrenes.

Experimental Section

General Information. All manipulations were carried out under a nitrogen or argon atmosphere, using standard Schlenk techniques. Benzene was dried by distillation from sodium benzophenone ketyl under nitrogen immediately prior to use. $Fe_2(CO)_9$ was obtained commercially (Aldrich) and was used as received. NMR spectra were recorded on a Bruker AVANCE 500 spectrometer: ^1H (500 MHz), ^{13}C (125.7 MHz). Infrared spectra were recorded on a Bruker IFS25 FT-IR spectrometer, as KBr discs or in solution phase using KBr cells equipped with PTFE spacers giving a path length of 0.1 mm. The solutions were introduced into the cell via a syringe. The opening of the cells were then sealed with 5 mm white PTFE stoppers. Mass spectra were recorded on a Finnigan 3300 gas chromatography−mass spectroscopy system using methane as a carrier gas for chemical ionization or electron impact (EI) at 70 eV. FAB or LSI mass spectra and exact mass measurements were done on a Kratos Concept-H instrument using perfluorokerosene as the standard. Elemental analyses were performed by Canadian Microanalytical Services Ltd., Vancouver, B.C. UV−vis spectra were recorded on a Cary 5 UV−vis−NIR spectrometer in the stated solvents. Melting points were determined on a Reichert 7905 melting point apparatus integrated to an Omega Engineering Model 199 chrome-alumel thermocouple. Silica gel (SiGel) refers to Merck silica gel, 60−200 mesh, deactivated with 5% water (by weight). NMR assignments were made on the basis of COSY, NOESY, DEPT, and long- and short-range HMQC 2D experiments. For NMR data, H-1,2 means H-1 and H-2, while H-1/2 means H-1 or H-2.

Reaction of Adduct 10 with $Fe_2(CO)_9$ at Room Temperature: Complex 6. A solution of adduct **10** (100 mg, 0.243 mmol) and $Fe_2(CO)_9$ (200 mg, 0.548 mmol) in dry benzene (15 mL) was stirred under argon at 20 °C in the dark for 18 h. The mixture was then filtered directly through a column of Si gel (10 cm) using benzene as eluant. The intense reddish-green solution was evaporated in the dark, and the residue was chromatographed on Si gel using hexane as eluant. The first red band yielded 20 mg (21%) of benzannulene **9** as red crystals. The second grass green band yielded 78 mg (60%) of complex **6**, mp ∼60 °C (dec color changed to reddish); ^1H NMR (C_6D_6) δ 8.31 (d, J = 1.4 Hz, 2H, H-3,6), 8.26 (d, J = 1.4 Hz, 2H, H-1,8), 8.21 (s, 2H, H-4,5), 5.97 and 5.91 (s, 1H each, H9,12), 3.29 (d, J = 5.1 Hz, 1H, H10/11), 3.04 (d, J = 5.1 Hz, 1H, H11/10), 1.61 and 1.60 (s, 9H each, $C(CH_3)_3$); −3.01 and −3.17 (s, 3H each, internal CH_3); ^{13}C NMR (C_6D_6) δ 211.2 (CO), 146.4 and 146.2 (C-7/2), 138.2 and 138.1 (C-3a/5a), 136.2 and 136.1 (C-12a/12f), 128.7 and 128.2 (C-12b/12e), 125.6 and 125.5 (C-4/5), 122.4 and 122.3 (C-3/6), 116.1 and 115.5 (C-1/8), 81.43 and 81.38 (C-9/12), 59.6 and 59.5 (C-10/11), 36.4 and 36.3 (2, 7-*C*$(CH_3)_3$), 34.0 and 32.4 (C-12c/12d), 32.3 and 32.1 (2, 7-C(*C*$H_3)_3$), 17.0 and 15.4 (12c, 12d-*C*H_3); UV−vis (cyclohexane) λ_{max} (ϵ_{max}) nm 207 (33 900), 361 (60 500), 387 (44 700), 453 (7340),

467 (7050), 528 (394), 577 (425), 641 (816); IR (KBr) 2082, 2021, 1991, 1968, 885, 655, 626, 605 cm^{-1}; (CH_2Cl_2 solution) 2083, 2008, 1976 (shoulder) cm^{-1}; LSI MS *m*/*z* 578.1 (M^+); HRMS calcd for $C_{34}H_{34}O_5Fe$ 578.1756, found 578.1754.

Reaction of Adduct 10 with $Fe_2(CO)_9$ in Refluxing Benzene. A solution of adduct **10** (600 mg, 1.46 mmol) and $Fe_2(CO)_9$ (1.15 g, 3.21 mmol) in dry benzene (50 mL) was stirred under argon under reflux in the dark for 2 h. After cooling, the mixture was filtered through Al_2O_3 (10 cm) using additional benzene (100 mL) as eluant. The intense red solution was evaporated in the dark. The solid was re-extracted with benzene (100 mL), and the solution was re-evaporated in the dark. The resulting red residue was chromatographed over Si gel using hexane as eluant. The first red band yielded 402 mg (70%) of benzannulene **9** as red crystals. The second dark green band yielded 77 mg (10%) of mono(tricarbonyliron) benzannnulene complex **7**. The third orange band yielded 118 mg (12%) of bis(tricarbonyliron) benzannnulene complex **8**. The fourth dark green band yielded 12 mg (1.5%) of complex **6**.

Complex **7**: mp 192−193 °C; ^{1}H NMR (C_6D_6) δ 7.41 (dd, $J_{9,10}$ = 8.0 Hz, $J_{9,11}$ = 1.4 Hz, 1H, H-9), 7.19 (dd, $J_{12,11}$ = 8.1 Hz, $J_{12,10}$ = 1.3 Hz, 1H, H-12), 6.97 (td, $J_{11,12}$ = 8.1 Hz, $J_{11,10}$ = 7.0 Hz, $J_{11,9}$ = 1.4 Hz, 1H, H-11), 6.91 (td, $J_{10,9}$ = 8.0 Hz, $J_{10,11}$ = 7.3 Hz, $J_{10,12}$ = 1.3 Hz,, 1H, H-10), 6.38 (d, J = 1.2 Hz, 1H, H-8), 5.73 (s, 1H, H-6), 5.58 (d, $J_{1,3}$ = 1.4 Hz, 1H, H-1), 5.29 (dd, $J_{5,4}$ = 5.7 Hz, J = 0.7 Hz, 1H, H-5), 5.11 (d, $J_{4,5}$ = 5.7 Hz, 1H, H-4), 3.67 (d, $J_{3,1}$ = 1.4 Hz, 1H, H-3), 2.47 (s, 3H, 12d-CH_3), 2.01 (s, 3H, 12c-CH_3), 1.10 (s, 9H, 2-C(CH_3)$_3$), 1.03 (s, 9H, 7-C(CH_3)$_3$); ^{13}C NMR (C_6D_6) δ 212.3 (CO), 145.9 (C-7), 144.3 (C-5a), 144.2 (C-3a), 140.9 (C-12e), 136.4 (C-12a), 134.6 (C-12f), 128.3 (C-11), 127.3 (C-10), 126.4 (C-12), 125.1 (C-9), 121.3 (C-5) 121.2 (C-6), 117.8 (C-8), 112.7 (C-4), 108.5 (C-2), 80.7 (C-1), 78.6 (C-12b), 64.1 (C-3), 44.4 (C-12c), 43.7 (C-12d), 34.8 (7-*C*(CH_3)$_3$), 34.3 (2-*C*(CH_3)$_3$), 30.5 (2-C(*C*H_3)$_3$), 29.3 (7-C(*C*H_3)$_3$), 27.5 (12c-*C*H_3), 27.1 (12d-*C*H_3); UV−vis (cyclohexane) λ_{max} (ϵ_{max}) nm 323 (30 600), 420 sh (∼8000), 500−600 tail (∼700); IR (KBr) 2032, 1977, 1954, 761, 611, 599, 552 cm^{-1}; (CH_2Cl_2 solution) 2032, 1972, 1962 cm^{-1}; EI-MS *m*/*z* 534 (M^+). Anal. Calcd for $C_{33}H_{34}O_3Fe$: C, 74.16; H, 6.41. Found: C, 74.20; H, 6.59.

Complex **8**: mp 203 °C (dec); ^{1}H NMR (C_6D_6) δ 7.40 (dd, $J_{12,11}$ = 7.8 Hz, $J_{12,10}$ = 1.4 Hz, 1H, H-9), 7.27 (dd, $J_{9,10}$ = 8.1 Hz, $J_{9,11}$ = 1.2 Hz, 1H, H-12), 7.07 (ddd, $J_{10,9}$ = 8.1 Hz, $J_{10,11}$ = 7.2 Hz, $J_{10,12}$ = 1.4 Hz,, 1H, H-11), 6.97 (ddd, $J_{11,12}$ = 7.8 Hz, $J_{11,10}$ = 7.2 Hz, $J_{11,9}$ = 1.2 Hz, 1H, H-10), 5.54 (dd, $J_{4,5}$ = 5.3 Hz, $J_{4,5}$ = 0.5 Hz, 1H, H-5), 5.52 (d, J = 1.6 Hz, 1H, H-1), 5.47 (dd, $J_{5,4}$ = 5.3 Hz, J = 0.5 Hz, 1H, H-4), 5.00 (d, J = 1.8 Hz, H-8), 3.89 (d, J = 1.4 Hz, 1H, H-3), 3.78 (d, J = 1.3 Hz, 1H, H-6), 1.67 (s, 3H, 12d-CH_3), 1.12 (s, 9H, 2-C(CH_3)$_3$), 1.02 (s, 9H, 7-C(CH_3)$_3$), 0.20 (s, 3H, 12c-CH_3); ^{13}C NMR (C_6D_6) δ 214.7 and 212.8 (CO), 146.4 (C-3a), 145.3 (C-5a), 139.4 (C-12f), 138.8 (C-12a), 129.1 (C-9), 128.5 (C-11), 127.6 (C-10), 126.1 (C-12), 116.0 (C-5), 113.6 (C-4), 108.9 (C-2), 103.5 (C-7), 101.3 (C-12e), 86.3 (C-8), 79.02 (C-1) 79.00 (C-12b), 63.9 (C-6), 62.9 (C-3), 43.2 (C-12c), 42.4 (C-12d), 34.5 (7-*C*(CH_3)$_3$), 34.3 (2-*C*(CH_3)$_3$), 30.8 (12d-*C*H_3), 30.50 (2-C(*C*H_3)$_3$), 30.48 (7-C(*C*H_3)$_3$), 26.5 (12c-*C*H_3); UV−vis (cyclohexane) λ_{max} (ϵ_{max}) nm 302 (20 300), 343 (20 000), ∼470 sh (∼4000), tail to 600 (∼200); IR (KBr) 2032, 2025, 1956, 618, 600 cm^{-1}; (CH_2Cl_2 solution) 2037, 2027, 1963 cm^{-1}; EI-MS *m*/*z* 674 (M^+). Anal. Calcd for $C_{36}H_{34}O_6Fe_2$: C, 64.12; H, 5.08. Found: C, 63.85; H, 5.08.

X-ray Crystallography. Crystals of compound **7** (**8**) were removed from the flask and covered with a layer of hydrocarbon oil. A suitable crystal was selected, attached to a glass fiber, and placed in the low-temperature nitrogen stream.[23] Data for both **7** and **8** were collected at 87(2) K using a Bruker/Siemens SMART APEX instrument (Mo Kα radiation, λ = 0.71073 Å) equipped with a Cryocool NeverIce low-temperature device. Data were measured using omega scans of 0.3° per frame for 10 s for **7** and **8**, and a full sphere of data was collected. A total of 2450 frames were collected with a final resolution of 0.83 Å. The first 50 frames were re-collected at the end of data collection to monitor for decay. Cell parameters were retrieved using SMART[24] software and refined using SAINTPlus[25] on all observed reflections. Data reduction and correction for *Lp* and decay were performed using the SAINTPlus software. Absorption corrections were applied using SADABS.[26] The structure was solved by direct methods and refined by least-squares methods on F^2 using the SHELXTL program package.[27] The structure was solved in the space group *P*2(1)/*n* (*Pbca*) by analysis of systematic absences. All non-hydrogen atoms were refined anisotropically. No decomposition was observed during data collection. Details of the data collection and refinement are given in Table 1. Further details are provided in the Supporting Information.

Acknowledgment. We thank the Natural Sciences and Engineering Research Council of Canada and the University of Victoria for support of this work. The Bruker (Siemens) SMART APEX diffraction facility was established at the University of Idaho with the assistance of the NSF-EPSCoR program and the M. J. Murdock Charitable Trust, Vancouver, WA.

Supporting Information Available: A cif file containing both **7** and **8**, Table S1, and NMR spectra for **6**, **7**, and **8** are available free of charge via the Internet at http://pubs.acs.org.

OM0700112

(23) Hope, H. *Prog. Inorg. Chem.* **1994**, *41*, 1.
(24) *SMART*, v.5.626, Bruker Molecular Analysis Research Tool; Bruker AXS: Madison, WI, 2002.
(25) *SAINTPlus*, v. 6.45a, Data Reduction and Correction Program; Bruker AXS: Madison, WI, 2003.
(26) *SADABS*, v.2.01, Empirical Absorption Correction Program; Bruker AXS Inc.: Madison, WI, 2004.
(27) Sheldrick, G. M. *SHELXTL*, v. 6.10, Structure Determination Software Suite; Bruker AXS Inc.: Madison, WI, 2001.